International Journal of Nanoelectronics and Materials
IJNeaM
ISSN 1985-5761 | E-ISSN 2232-1535

Phyto-reduction of graphene oxide into reduced graphene oxide using *centella asiatica* extract for downstream applications

A. Khazali[b], S Taniselass [a,b] *, Subash C. B. Gopinath [c,d], K. Ananda-Rao[e], M. K. Md. Arshad[a,b]

[a]*Institute of Nano Electronic Engineering, Universiti Malaysia Perlis (UniMAP), Kangar 01000, Malaysia*
[b]*Faculty of Electronic Engineering & Technology, Universiti Malaysia Perlis (UniMAP), Arau 02600, Malaysia*
[c]*Department of Neonatology, Saveetha Medical College and Hospital, Saveetha Institute of Medical and Technical Sciences, Chennai 602105, Tamil Nadu, India*
[d]*Faculty of Chemical Engineering & Technology, Universiti Malaysia Perlis (UniMAP), Arau 02600, Perlis, Malaysia.*
[e]*Faculty of Electrical Engineering & Technology, Universiti Malaysia Perlis (UniMAP), Arau 02600, Malaysia*
∗ Corresponding author. Tel.: +0-000-000-0000; fax: +0-000-000-0000; e-mail: steven@unimap.edu.my

Received 12 February 2026, Revised 11 March 2026, Accepted 19 March 2026

ABSTRACT

Green phyto-synthesis represents an environmentally sustainable approach that employs eco-friendly methods and materials to produce various substances, minimizing the use of hazardous chemicals and reducing the overall ecological footprint. The central focus of this research is the utilization of *Centella asiatica* (*C. asiatica*) to reduce Graphene Oxide (GO) into reduced Graphene Oxide (rGO). Two rGO samples, designated as rGO1 and rGO2 were synthesized at varying concentrations of *C. asiatica* extract to investigate the influence of reduction parameters on the desired material. Techniques such as Scanning Electron Microscopy (SEM), High-Power Microscopy (HPM), UV-Vis, Raman, Fourier Transform Infrared Spectroscopy (FTIR) and Four-Point Probes were used to analyze the as-synthesized materials. A mild reduction was occurred under eco-friendly environment where the UV–Vis spectral showed a shift of an absorption peak from 230 nm (GO) to ~241nm (rGO1) and ~250 nm (rGO2), respectively. The microscopy images from HPM and SEM revealed a wavy-like rGO nanoflakes is observed and the restoration of sp^2 carbon network with minor shifts of G-band indicated by Raman spectral. The reduction and removal of oxygen moieties are further supported by FTIR analyses. Meanwhile, decreased in electrical resistivity from 23.50 Ω·m (GO) to 7.45 Ω·m (rGO2), indicates an improved conductivity, thus supporting the removal of oxygen groups. In summary, the test results confirm the green reduction of GO to produce rGO by C. asiatica is effective and facilitates to produce a structurally stable nanomaterials and conductive that are suitable for electronic and bio-sensing applications. NOTE: The header and footer of this manuscript is not following the provided guideline, please check again.

Keywords: *Graphene oxide nanomaterial, Reduced graphene oxide, Centella asiatica, Nanostructure, Green phyto-synthesis*

1. INTRODUCTION

Graphene derivatives, a two-dimensional (2D) carbon atoms in honeycomb lattice have emerged as a groundbreaking nanomaterial with remarkable properties that attracting scientific and industrial communities of its potential use [1]. Graphene composed of a single sheet and the carbon atoms are organized in a hexagonal lattice and exhibits extraordinary mechanical strength, outstanding electrical conductivity, and exceptional thermal conductivity. Because of these properties, graphene is a viable option for a wide range of applications, such as energy storage, electronics, sensors, and catalysis [2].

Graphene Oxide (GO) is an oxidized form of graphite, and it serves as a precursor to graphene. GO contains functional groups with oxygen moieties, which give it hydrophilicity and makes it easier to dissolve in aqueous solutions. However, GO's properties differ significantly from pristine graphene, and a reduction process, is essential to restore graphene-like features [2]. Traditional reduction techniques, including chemical and thermal methods, have been widely employed due to their efficacy and accessibility. However, the leverage of hazardous chemicals within these synthesis steps raises concerns in relation to sustainability and environmental perspective [3]. To address these limitations, green synthesis methods have emerged, employing environmentally benign reagents such as plant extracts and biological agents. These techniques support sustainable practices in the field of graphene manufacturing and present a viable alternative for traditional methods [4].

Among various plant-based reducing agents, *Centella asiatica (C. asiatica)* has garnered a particular interest owing to its rich profile of bioactive substances, including flavonoids, triterpenoids, saponins and essential oils [3]. The bioactive substances present in the extract of *C. asiatica* are essential for the reduction of GO. It is thought that triterpenoids act as reducing agents that help to remove oxygen-containing functional groups from the surface of GO [3],[5]. Moreover, saponins which are amphiphilic enhance the dispersion of GO sheets in the extract solution and facilitating the interaction between GO and the reducing agents. The antioxidant properties of this bioactive substances contribute to the structural stability

of the *C. asiatica* extract whereby flavonoids plays vital role in maintaining the stability. Furthermore, the preparation of *C. asiatica* extract is straightforward and less cost becoming an attractive option as a reducing agent [6]. The GO reduction can be tuned by optimizing the *C. asiatica* concentration which enables the modification of rGO properties to support various potential applications. Hence, the rGO derived from phyto-green reduction is highly potential for biosensors development and in health-related application because of free from toxicity procedures. The resulting green rGO with its oxygen groups are used to develop high sensitivity biosensors such as glucose biosensor, immunosensors and DNA biosensors for monitoring various diseases in non-invasive ways [7].

Several researchers have attempted to use the *C. asiatica* for the reduction of GO. Recently, Manjula et al. demonstrated that reduced graphene oxide blended with cadmium oxide exhibited improved antibacterial and photocatalytic properties. However, the GO reduction was carried by using roasted leaves, which may have resulted in the significant loss of bioactive compound [8]. Suganya et al. synthesized reduced graphene oxide (rGO) decorated with a lead sulfide/cadmium oxide nanocomposite using fresh C.asiatica leaf juice extract with volume proportions for the reduction but without considering the concentration [9]. Meanwhile, Vinutha et al. used the CA extract powder mixed with GO to form carbonaceous composite electrode materials for electrochemical applications, though the reduction was not tested [10].

In this study, *C. asiatica* extract was employed to reduce the GO and optimized the reduction process by varying its concentrations. The reduction efficiency and the resulting nanomaterial properties were analyzed and evaluated. The as-synthesized rGO samples were characterized using High-Power Microscopy (HPM), Scanning Electron Microscopy (SEM), Ultraviolet Visible (UV–Vis), Raman, and Fourier Transform Infrared (FTIR) spectroscopies to evaluate the morphological, structural and chemical transformations. Furthermore, a Four-Point Probe was used to identify the electrical characteristics of the as-prepared rGO samples. The findings from this study is aimed to drive an eco-friendly and sustainable graphene-based nanomaterial for next generation biosensing applications.

2. METHODOLOGY

The preparation of *C. asiatica* extract, reduction of GO and the subsequent characterization steps were discussed in the following sub-topics.

2.1. Preparation of *C. asiatica* Extract

A handful *C. asiatica* leaves, locally known as “Pegaga,” was procured from a local farm in Perlis, Malaysia to ensure material consistency. Then, the leaves were thoroughly washed and rinsed with tap water to eliminate any dirt and soil particles without any chemicals usage [Figure 1(a)]. This ensures that the leaves are clean and safe to be used. It also prevents contaminants and other particles from affecting the results.

A 50 grams of the fresh C. *asiatica* leaves were weighed using a precision scale. The fresh leaves were then placed under sunlight to dry, a process that takes about 5 days and subsequently were stored in a closed container until further use. This method allows for the natural elimination of water content and to protect the integrity of the bioactive compounds. Next, the weight of the dried leaves was re-assessed to ensure the water content/moisture had been removed. Initially, 50 grams of fresh leaves were measured and after the drying process the weight was reduced to 12 grams, indicating a 38 grams of water content/moisture had been removed. Then, the dried C. *asiatica* leaves were grinded using electric grinder and filtered to produce a fine powder. The final weight of 9 grams of fine powder were collected for further process. The remaining 3 grams of loss was from filtering steps where it consists of coarse fibers and filtered stolon as-well as other unwanted parts.

2.2. Preparation of CA and GO Solution

The dried powdered of C. *asiatica* extract was then used to prepare an aqueous solution of varying concentration. Specifically, 80 mg of C. *asiatica* powder was dispersed in 40 mL of deionized (DI) water. Next, the mixtures were stirred and heated at 60 °C for 30 minutes using a magnetic stirrer to facilitate the diffusion occurs. After heating and stirring, the solutions were allowed to cool naturally to room temperature. Several samples with various concentrations of *C. asiatica* were prepared, including 2-, 4-, 6-, 10-, and 20- mg/ml as shown in Figure 1 (b). The color changes were observed before selecting the amount of 10 mg/ml for further analysis.

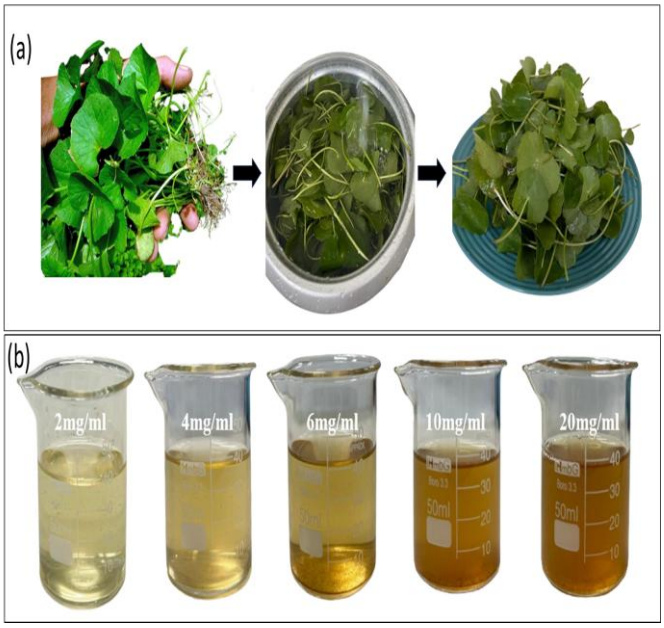

Figure 1. (a) Preparation of *C. asiatica* leaves, (b) and the color comparison of extracted solution at various amounts

Next, GO solution was prepared where 20 mg GO powder was dispersed in 40 mL of DI water to prepare a 0.5 mg/mL solution. The mixture was stirred thoroughly to ensure even dispersion and followed by sonication bath for 30 minutes. Once the sonication was completed, the GO solution was allowed to cool down naturally to room temperature.

2.3. Reduction of Graphene Oxide Using *C. asiatica*

For the green reduction process, two distinct C. *asiatica* extract amounts were selected based on the color variation, where rGO1 refers to GO reduced with 2 mg/ml of C. *asiatica* extract, and rGO2 refers to GO reduced with 10 mg/ml of C. *asiatica* extract. An equal volume (v/v) of C. *asiatica* and GO solutions were mixed at 1:1 ratio, to ensure an equivalent volume of composition were used for the reduction process. Then, the mixture was continuously stirred at 80 °C using hot plate with a magnetic stirrer for 60 minutes. After the reduction, the samples were allowed to cool down naturally before transferred to vial, concluding the rGO synthesis phase.

2.4. Preparation of Commercially Reduced Graphene Oxide (C-rGO)

A commercially reduced graphene oxide (C-rGO) was prepared to benchmark the phyto reduction and for comparative analysis. Hence, a C-rGO suspension with a concentration of 0.5 mg/mL was prepared in DI water, maintaining the same concentration as prepared previously [11]. Then, the mixture was sonicated for 30 minutes to achieve a uniform suspension. After sonication step, the C-rGO suspension was allowed to cool down naturally at room temperature before transferred to vial for further analysis.

2.5. Characterization Techniques

Characterization plays a major role to understand graphene derivative properties and to determine a right application for the nanomaterials. Hence, an advanced characterization technique is required to evaluate the 2D nanomaterial. In this work, SEM, HPM, UV-Vis, Raman, FTIR spectroscopies and Four Point Probes are employed for comprehensive analysis of the as-prepared nanomaterial. HPM is used for characterizing the material surface morphology at various magnifications. A droplet from the as-prepared samples of GO, rGO1, rGO2 and C-rGO were drop-casted onto glass slide for HPM analysis. The glass slides were cleaned using isopropyl alcohol (IPA) before drop cast the samples. Then, the samples were heated at 60 °C on the hot plate to enables the sample adhesion. Furthermore, SEM is used to observe a high-resolution of surface morphology and other structural features.

UV–Vis spectroscopy is used for validating the reduction process. The optical spectral analysis was conducted for a range of 200 to 450 nm of wavelength. The range of 200 to 450 nm was chosen to observe any absorption peaks where graphene oxide sample are interacts optically with lights within this range of wavelengths.

Structural and electrical properties were further analyzed using Raman and Four-Point Probe measurements. Raman spectroscopy was used to recognize the graphene nanomaterial based molecular structure by identifying the D- and G-bands. A shift of G-band can indicate changes in the degree of graphitization while a shift in D-band can reflect the defects structure in the material [12]. The ratio between D and G band intensities (ID/IG), can indicate the extent of distortion in graphitic sheets. A high ID/IG values simply indicate a greater disorder [13]. The electrical measurement was performed using a Four-Point Probe setup, to measure the sheet resistance of the as-prepared samples. The thin films samples were measured repeatedly and checked for any drift. The probes were repositioned to different sample areas to ensure the measurement is uniform and stable. All data, including applied current, measured voltage, probe spacing, and temperature, were cautiously recorded.

Meanwhile, FTIR was employed to detect the oxygen functional groups of the as-prepared samples. FTIR helps to understand the presence or changes in oxygen-containing groups that occurs during the reduction process. The as-prepared samples, consisting of GO and rGO2 (is selected based on UV-Vis results), was further used for FTIR spectral analysis.

3. RESULTS AND DISCUSSION

Proper characterization of GO and rGO are essential to validate the reduction process and assess the impact of green reduction. The use of *C. asiatica* as a reducing agent is warranting a comparison of its effectiveness with other green reducing agents.

3.1. UV-Vis Spectroscopy

Figure 2 shows UV-Vis spectral analysis for the 4 samples of GO, rGO1, rGO2 and C-rGO. The absorption peak of GO was observed at 230 nm, within the expected range, validating its characteristic absorption behavior in agreement with Mahmoud et al. [14]. Besides that, the reference sample, C-rGO, showed a peak at 272 nm, consistent with Priliana et al. [5]. Following with the reduction validation of rGO1 and rGO2, the expectation was a red shift, and the shift occurs around 241 nm and 249 nm, respectively indicating a mild green reduction were occurred [15]. The result further confirms that rGO2 samples were reduced better than rGO1. It confirms the restoration of the sp^2 hybridized carbon network due to the removal of oxygen-bearing functional groups in rGO2 [16]. For rGO1, the shift is too minimal about 10 nm compared to GO due to a low concentration of *C. asiatica* (2 mg/mL) were used. This further suggest that a higher concentration of *C. asiatica* (> 10 mg/mL) is recommended to reduce 0.5

mg/mL of GO suspension at eco-friendly environment without any high-tech tools.

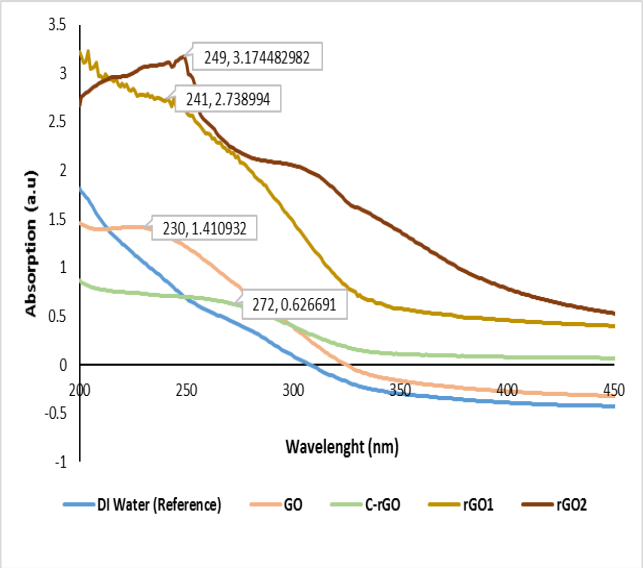

Figure 2. UV-Vis Spectra of GO, C-rGO rGO1 and rGO2. Values indicated at peak maxima.

3.2. High-Power Microscopy (HPM)

Figure 3 shows HPM analysis and it revealed clear differences in the morphology of GO, C-rGO, rGO1 and rGO2. GO and distinctly visible at a 50X magnification, and its identity is verified by its bright (white) appearance. The well-defined edges of GO flakes signify clear boundaries for each individual flake. These flakes are characterized as irregular sheets with few layers, indicating a limited layer count and an uneven structure [16], [17].

C-rGO nanoflakes are visible by its bright (white) appearance, observed at 50X magnification. The brightness verifies the formation of multi layered/thin film nanosheets where a dull flake indicates a reduced number of layers [11]. HPM can predicts the variations of nanoflakes thickness by light reflections. The color contrast between bright white, dark and dull flakes are attributed to the light reflection by an optical microscope which explains the corresponding changes in the rGO nanosheets thickness [17]. In rGO1, a limited presence of white nanoflakes is observed along with some blueish and black spots flakes presents in the deposition area. This indicates a noticeable change in surface roughness when comparing GO. However, the surface roughness of C-rGO is clearly visible than GO, aligning with findings from prior research where large graphitization occurs in the commercially produced rGO [16]. Conversely, for rGO2, more bright white flakes were observed in the sample when compared to rGO1 and GO. The presence of densely packed bright white nanoflakes is due to the removal of oxygen groups This further indicates that there is a restoration of sp^2 hybridized carbon network that suggest more reduction happened at rGO2 when compared to rGO1.

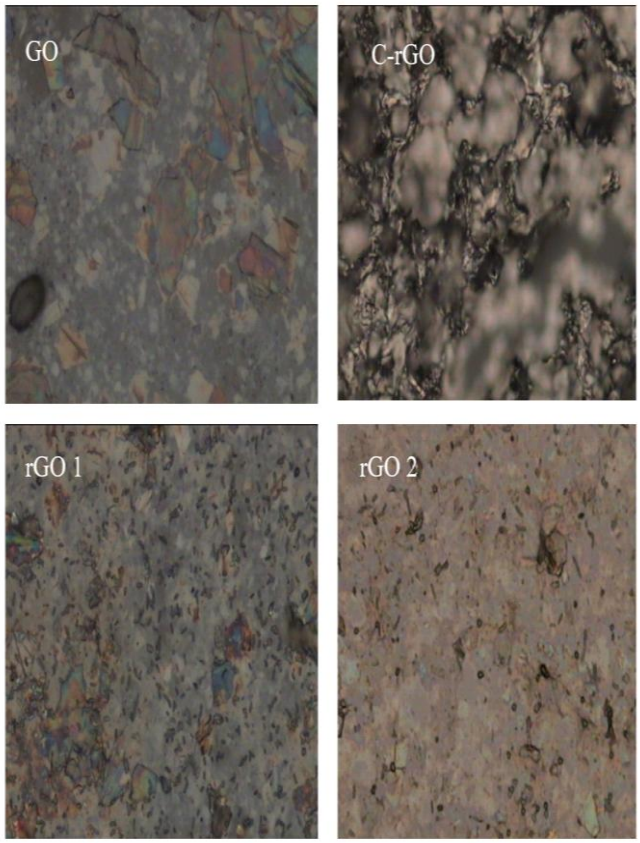

Figure 3. HPM surface morphology of GO, C-rGO, rGO1 and rGO2 at a 50X magnification.

3.3. RAMAN Spectroscopy

For Raman analysis, four samples were analyzed, focusing on GO, rGO1, rGO2, and a reference sample of C-rGO. In Figure 4 (a), the GO sample exhibited a notable D-band peak at 1338 cm^{-1} and a significant G-band peak at 1578 cm^{-1}. These results are indeed within the expected range for GO. For rGO1, the D-band peak shifted to 1336 cm^{-1}, indicating a decrease, while G-band peak was observed at 1601 cm^{-1}. For rGO2, the D-band peak shifted to 1349 cm^{-1}, with slight increase, while the G-band peak was observed at 1600 cm^{-1}. Meanwhile, D- and G-band peaks for C-RGO was observed at 1348 and 1566 cm^{-1}, respectively. Analysis shows that for D-band, there is not much change among GO, rGO1, and rGO2 indicating that all samples are consistent with defects. However, the slight shift with G-band indicates a change in sp^2 hybridized carbon atoms due to the reduction process. The shift towards a higher range suggests the restoration of electronic conjugation between graphene layers and restacking, as the expulsion of oxygen functionalities allows the rGO to associate and restack [19]. Meanwhile, the degree of disorder (ID/IG ratio), Table 1 shows that the differences among all samples are negligible. While some research mentions a decrease in the ID/IG ratio from GO to rGO, indicating the removal of oxygen-containing functional groups [13], the GO used had a ratio to be below 1, indicates the sample have a low number of defects

Table 1. Degree of Disorder (ID/IG)

Material	ID/IG
GO	0.848
rGO1	0.834
rGO2	0.843
C-rGO	0.860

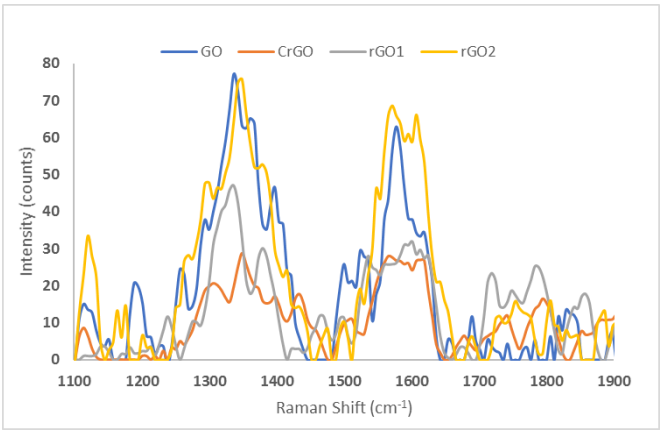

Figure 4. Raman spectra of GO, C-rGO, rGO1 and rGO2. The spectra were overlapped for comparison.

3.4. Four-Point Probe Electrical Characterization

The four-point probe technique was employed to evaluate the electrical conductivity of the as-prepared samples (GO, rGO1 and rGO2). Figure 5 plots reveal that the resistivity of the rGO2 sample is significantly smaller than that of rGO1 and GO, indicating superior electrical conductivity. The currents values demonstrate a distinct difference for the GO, rGO1, and rGO2 samples. The GO sample has highest resistivity at 23.501 Ω·m, indicating higher resistance to electrical current among the samples. The higher resistivity is due to the presence of oxygen functional groups in the nanoflakes that disrupts the graphene conductive networks [20]. Moreover, the resistivity of rGO1 is reduced to 14.121 Ω·m compared to GO. This decreases in resistivity indicates an improved electrical conductivity due to the partial removal of oxygen groups that can leads to the restoration of the graphene structure [20]. Furthermore, rGO2 sample exhibits the lowest resistivity at 7.453 Ω·m, which indicates the highest electrical conductivity among the samples. The significant reduction in resistivity is attributed to the more complete reduction process occurs that facilitates the removal oxygen groups and the restoration of the graphene conductive networks [21].

By analyzing the I-V curve plots and the corresponding resistivity values, it is evident that the reduction of GO to rGO significantly improves the material's electrical properties. Furthermore, it highlights the green reduction using C. *asiatica* is effective and enhancing the electrical properties of graphene oxide

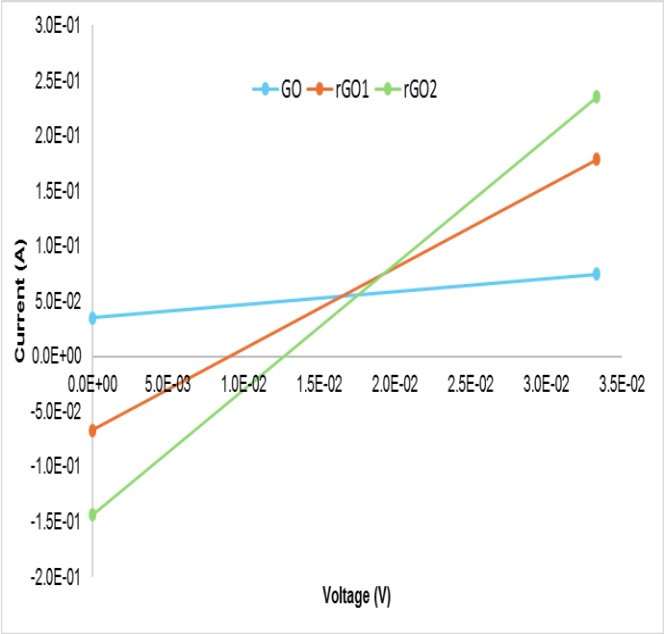

Figure 5. I-V characteristics of GO, rGO1, and rGO2.

3.5. Fourier Transform Infrared Spectroscopy (FTIR)

Figure 6 shows the FTIR spectral analysis of the as-reduced samples which revealed the impact on the reduction of different amounts of the reducing agent and the resultant functional groups. Specifically, Figure 6 (a) shows the FTIR peaks for rGO1 where a broad peak around 3376.12 cm^{-1} is observed which indicates the presence of hydroxyl groups (-OH). The other peaks such as 1538.82 cm^{-1} and 1505.8 cm^{-1} pointing to the retention of aromatic rings and some residual oxygen-containing groups. Figure 6 (b) displays the FTIR peaks for rGO2, showing similar broad peaks around 3379.44 cm^{-1} for hydroxyl groups or adsorbed moisture, and additional peaks at 2335 cm^{-1} and 2125.2 cm^{-1} corresponding to alkyne (carbon-carbon triple bond (C≡C)) and nitrile groups (carbon-nitrogen triple bond (C≡N)), respectively. These peaks are absent in rGO1, indicating that the higher concentration of CA in rGO2 has introduced new functional groups and suggests a more complex reduction mechanism. Additionally, the C–H bending vibrations around 1389.3 cm^{-1} for rGO1 and 1382.6 cm^{-1} for rGO2 indicate the presence of methyl or methylene groups, pointing to residual organic functionalities in both samples. Figure 6 (c) compares both spectral of rGO1 and rGO2 to highlights the differences in their functional groups. The presence of a peak at 1638.22 cm^{-1} in rGO2 suggests better retention of aromatic structures which possibly due to the higher concentration of the reducing agent that promoting effective reduction. This analysis indicates that rGO2 has undergone a more extensive reduction process, resulting in the effective reduction of oxygen-containing groups and the introduction of new functionalities. Therefore, the higher concentration of *C. asiatica* in rGO2 enhances the reduction process, potentially improving the properties of rGO for specific applications.

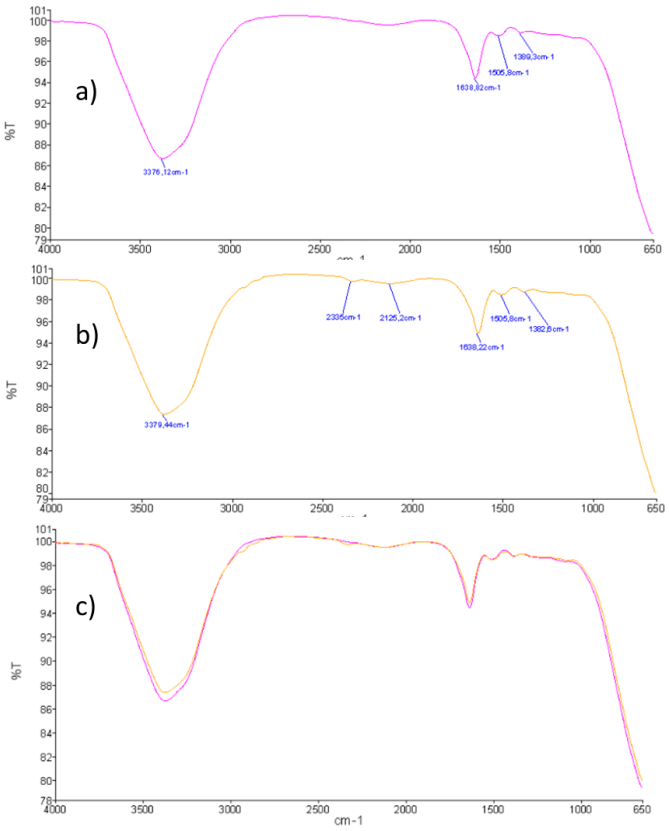

Figure 6. FTIR spectral of (a) rGO1; (b) rGO2; (c) Overlay comparison.

3.6. Scanning Electron Microscopy (SEM)

The surface morphology of rGO1 and rGO2 was further evaluated by using SEM and the captured images is shown in Figure 7 at a magnification of 1000x. In Figure 7 (a), rGO1 has larger lumped like plates compared to rGO2 as shown in Figure 7 (b). This is due to the less reduction and minimal restoration of sp^2 carbon, which explain larger graphene oxide plates still present. As a result, the graphene sheets crumple together, forming larger graphene plates [19]. However, the rGO2 shows a wavy-like sheets, more wrinkled with high porosity as can be seen in Figure 7(b). This can be attributed to the reduction of oxygen in the basal plane of the sp^2 carbon network. During the reduction, the lamellas self-assemble via van der Waals forces, leading to increased stacking (as seen in rGO2) [5].

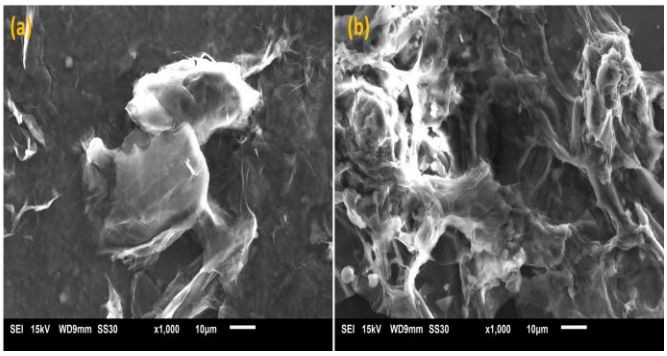

Figure 7. SEM images of (a) rGO1 and (b) rGO2 at 1000x magnifications

4. CONCLUSION

The as-prepared rGO samples were evaluated by the combination of microscopy imaging, spectroscopy analyses and electrical characterization which gives an insight into the morphology, structural and electrical properties of the material. The analyses further verified that *C. asiatica* extract effectively enhances the GO reduction, with rGO2 showing greater in morphological, structural integrity and electrical performance compared to rGO1. HPM shows both rGO1 and rGO2 exhibited bright white spot appearances, with rGO2 showing higher density of bright spots. Validation through UV-Vis spectroscopy confirmed reduction process, with rGO2 demonstrating a more pronounced shift, indicating a more effective reduction process with high amount of *C. asiatica*. The four-point probe technique demonstrates that reducing GO to rGO significantly enhances electrical conductivity. GO has the highest resistivity due to its oxygen content, while rGO shows much lower resistivity due to the removal of oxygen groups. This reduction process effectively improves the electrical properties of graphene-based materials, making rGO highly suitable for applications requiring high conductivity. Raman analysis further showed the structural changes induced by the reduction process, particularly in the shifting of the D-band and G-band peaks. Thus, the plant-based phyto-reduction approach using *C. asiatica* demonstrates a potential for producing high-quality rGO for the downstream electronic and sensing applications.

ACKNOWLEDGMENTS

The authors would like to acknowledge the support from the Fundamental Research Grant Scheme under a grant number of FRGS/1/2023/STG01/UNIMAP/02/2 from the Ministry of Higher Education Malaysia.

REFERENCES

[1] X. Chen, A. Bouhon, L. Li, F. M. Peeters, and B. Sanyal, "PAI-graphene: A new topological semimetallic two-dimensional carbon allotrope with highly tunable anisotropic Dirac cones," *Carbon*, vol. 170, pp. 477–486, Dec. 2020, doi: 10.1016/j.carbon.2020.08.012.

[2] R. Teixeira-Santos, S. Belo, R. Vieira, F. J. M. Mergulhão, and L. C. Gomes, "Graphene-based composites for biomedical applications: Surface modification for enhanced antimicrobial activity and biocompatibility," *Biomolecules*, vol. 13, no. 11, p. 1571, Oct. 2023, doi: 10.3390/biom13111571.

[3] "Facile synthesis of reduced graphene oxide using natural plant extracts as green reducing agents," *Journal of King Saud University – Engineering Sciences*, 2025. [Online]. Available: https://link.springer.com/article/10.1007/s44444-025-00007-9.

[4] Thokchom, B., Bhavi, S.M., Abbigeri, M.B. *et al.* Green synthesis, characterization and biomedical applications of *Centella asiatica*-derived carbon dots. *Carbon Lett.* **33**, 1057–1071 (2023). https://doi.org/10.1007/s42823-023-00505-3.

10.1016/j.jhazmat.2019.03.046.

[5] V. Priliana, C. Sucitro, R. Wijaya, V. B. Lunardi, S. P. Santoso, M. Yuliana, C. Gunarto, A. E. Angkawijaya, and W. Irawaty, "Reduction of graphene oxide using Citrus hystrix peels extract for methylene blue adsorption," Sustainability, vol. 14, no. 19, p. 12172, Oct. 2022, doi: 10.3390/su141912172.

[6] A. E. D. Mahmoud, M. Hosny, N. El-Maghrabi, and M. Fawzy, "Facile synthesis of reduced graphene oxide by Tecoma stans extracts for efficient removal of Ni(II) from water: Batch experiments and response surface methodology," Sustainable Environment Research, vol. 32, no. 1, Dec. 2022, doi: 10.1186/s42834-022-00131-0.

[7] J. Lee, J. Kim, S. Kim, and D. H. Min, "Biosensors based on graphene oxide and its biomedical application," Advanced Drug Delivery Reviews, vol. 105, pp. 275–287, Oct. 2016, doi: 10.1016/j.addr.2016.06.001.

[8] Manjula, N., Balu, A. R., Arunkumar, N., Devi, S. C., Sriramraj, M., Rajamani, V., & Vinith, A. "Water remediation and antibacterial characteristics of CdO, graphene oxide and reduced graphene oxide blended CdO nanoparticles–a comparative study" Chemistry of Inorganic Materials, 5, doi.org/10.1016/j.cinorg.2025.100090.

[9] Suganya, M., Balu, A. R., Devi, S. C., Usharani, K., Sriramraj, M., Devendran, K., & Adityan, S. "Centella asiatica Leaf Extract Mediated One-Pot Green Synthesized rGO Decorated PbS/CdO Nanocomposite for Catalytic Degradation of Methyl Violet from Wastewater and Resistance Against Bacillus subtilis and Pseudomonas aeruginosa Bacterial Strains," Water, Air, & Soil Pollution, 235(1), 14, 2024 doi.org/10.1007/s11270-023-06810-x.

[10] Vinutha, K., Divakara, M. B., Veena, K., Kumar, M. A., Ravikumar, C. R., Santosh, M. S., ... & Gurushantha, K. "Centella asiatica and its carbonaceous composites as novel materials for photocatalytic and electrochemical applications," Materials Today: Proceedings, 46, 5936-5941. 2021, doi.org/10.1016/j.matpr.2020.09.266.Thokchom.

[11] S. Taniselass, M. K. M. Arshad, S. C. B. Gopinath, and M. M. Ramli, "Self-assembled reduced graphene oxide nanoflakes assisted by post-sonication boosted electrical performance in gold interdigitated microelectrodes," Journal of Colloid and Interface Science, vol. 577, pp. 345–354, Oct. 2020, doi: 10.1016/j.jcis.2020.05.070.

[12] M. Mahmudzadeh, H. Yari, B. Ramezanzadeh, and M. Mahdavian, "Highly potent radical scavenging–antioxidant activity of biologically reduced graphene oxide using nettle extract as a green biogenic amine-based reductant source instead of hazardous hydrazine hydrate," Journal of Hazardous Materials, vol. 371, pp. 609–624, Jun. 2019, doi:

[13] M. S. Amir Faiz, C. A. Che Azurahanim, S. A. Raba'ah, and M. Z. Ruzniza, "Low-cost and green approach in the reduction of graphene oxide (GO) using palm oil leaves extract for potential industrial applications," Results in Physics, vol. 16, Mar. 2020, doi: 10.1016/j.rinp.2020.102954.

[14] A. E. D. Mahmoud, M. Hosny, N. El-Maghrabi, and M. Fawzy, "Facile synthesis of reduced graphene oxide by Tecoma stans extracts for efficient removal of Ni(II) from water: Batch experiments and response surface methodology," Sustainable Environment Research, vol. 32, no. 1, Dec. 2022, doi: 10.1186/s42834-022-00131-0.

[15] F. C. Mascarenhas, N. Sykam, M. Selvakumar, and M. G. Mahesha, "Green reduction of graphene oxide using Indian gooseberry (amla) extract for gas sensing applications," Journal of Environmental Chemical Engineering, vol. 8, no. 2, Apr. 2020, doi: 10.1016/j.jece.2020.103712.

[16] L. A. Pérez, N. Bajales, and G. I. Lacconi, "Raman spectroscopy coupled with AFM scan head: A versatile combination for tailoring graphene oxide/reduced graphene oxide hybrid materials," Applied Surface Science, vol. 495, Nov. 2019, doi: 10.1016/j.apsusc.2019.143539.

[17] IEEE Malaysia Section, "Proceedings of the 2nd International Conference on Biomedical Engineering (ICoBE 2015), Penang, Malaysia, March 30–31, 2015," IEEE, 2015.

[18] R. M. N. M. Rathnayake, H. W. M. A. C. Wijayasinghe, H. M. T. G. A. Pitawala, M. Yoshimura, and H. H. Huang, "Synthesis of graphene oxide and reduced graphene oxide by needle platy natural vein graphite," Applied Surface Science, vol. 393, pp. 309–315, Jan. 2017, doi: 10.1016/j.apsusc.2016.10.008.

[19] N. J. Panicker and P. P. Sahu, "Green reduction of graphene oxide using phytochemicals extracted from Pomelo grandis and Tamarindus indica and its supercapacitor applications," Journal of Materials Science: Materials in Electronics, vol. 32, no. 11, pp. 15265–15278, Jun. 2021, doi: 10.1007/s10854-021-06077-0.

[20] S. Kumuda, U. Gandhi, U. Mangalanathan, and K. Rajanna, "Synthesis and characterization of graphene oxide and reduced graphene oxide chemically reduced at different time duration," Journal of Materials Science: Materials in Electronics, vol. 35, no. 9, Mar. 2024, doi: 10.1007/s10854-024-12393-y.

[21] A. Mitra et al., "Large enhancement of thermal conductivity of aluminum–reduced graphene oxide composites prepared by a single-step method," Oxford Open Materials Science, vol. 3, no. 1, 2023, doi: 10.1093/oxfmat/itac015.